REPORT

Mutations in *CAPN1* Cause Autosomal-Recessive Hereditary Spastic Paraplegia

Ziv Gan-Or,[1,2,3,15] Naima Bouslam,[4,15] Nazha Birouk,[5,15] Alexandra Lissouba,[6,7,15] Daniel B. Chambers,[8] Julie Vériepe,[6,7] Alaura Androschuck,[8] Sandra B. Laurent,[1,3] Daniel Rochefort,[1,3] Dan Spiegelman,[1,3] Alexandre Dionne-Laporte,[1,3] Anna Szuto,[1] Meijiang Liao,[6,7] Denise A. Figlewicz,[10] Ahmed Bouhouche,[4] Ali Benomar,[4] Mohamed Yahyaoui,[4] Reda Ouazzani,[5] Grace Yoon,[11,12] Nicolas Dupré,[13] Oksana Suchowersky,[14] Francois V. Bolduc,[8] J. Alex Parker,[6,9] Patrick A. Dion,[1,3] Pierre Drapeau,[6,7] Guy A. Rouleau,[1,2,3,*] and Bouchra Ouled Amar Bencheikh[1,6]

Hereditary spastic paraplegia (HSP) is a genetically and clinically heterogeneous disease characterized by spasticity and weakness of the lower limbs with or without additional neurological symptoms. Although more than 70 genes and genetic loci have been implicated in HSP, many families remain genetically undiagnosed, suggesting that other genetic causes of HSP are still to be identified. HSP can be inherited in an autosomal-dominant, autosomal-recessive, or X-linked manner. In the current study, we performed whole-exome sequencing to analyze a total of nine affected individuals in three families with autosomal-recessive HSP. Rare homozygous and compound-heterozygous nonsense, missense, frameshift, and splice-site mutations in *CAPN1* were identified in all affected individuals, and sequencing in additional family members confirmed the segregation of these mutations with the disease (spastic paraplegia 76 [SPG76]). *CAPN1* encodes calpain 1, a protease that is widely present in the CNS. Calpain 1 is involved in synaptic plasticity, synaptic restructuring, and axon maturation and maintenance. Three models of calpain 1 deficiency were further studied. In *Caenorhabditis elegans*, loss of calpain 1 function resulted in neuronal and axonal dysfunction and degeneration. Similarly, loss-of-function of the *Drosophila melanogaster* ortholog calpain B caused locomotor defects and axonal anomalies. Knockdown of *calpain 1a*, a *CAPN1* ortholog in *Danio rerio*, resulted in abnormal branchiomotor neuron migration and disorganized acetylated-tubulin axonal networks in the brain. The identification of mutations in *CAPN1* in HSP expands our understanding of the disease causes and potential mechanisms.

Hereditary spastic paraplegia (HSP) includes a rare group of neurological disorders with an estimated prevalence of 2–10/100,000 individuals in different populations.[1–3] HSP can be classified as pure or complicated on the basis of the clinical presentation. Pure HSP is characterized by progressive spasticity and weakness, limited to the lower limbs, and often manifests as deep-tendon hyperreflexia and the extensor plantar response. Additional often-reported features of the pure form are a hypertonic bladder and lower-limb sensory disturbances. Complicated HSP is accompanied by other neurological symptoms, including seizures, ataxia, intellectual disability, dementia, extrapyramidal symptoms, peripheral neuropathy (if other causes of peripheral neuropathy are ruled out), amyotrophy, optic atrophy, and others.[3,4] Although HSP can be debilitating, individuals with HSP often have a normal lifespan; therefore, post-mortem studies are not common, and neuropathological data are limited. However, the available information indicates that HSP is typically characterized by axonal degeneration of the descending corticospinal tract and ascending sensory fibers.[5] HSP is a genetically heterogeneous disease; currently, there are more than 70 known or suspected genes or genetic loci in which mutations have been suggested to cause HSP.[6,7] Some of the genes are exclusively associated with pure or complicated HSP; however, other genes are associated with both forms of HSP, indicating that other genetic or environmental factors can modify the disease course. HSP can be inherited in an autosomal-dominant (AD-HSP [MIM: 182601]), autosomal-recessive (AR-HSP [MIM: 604360]), or X-linked (XL-HSP) manner. Mutations in *SPAST* (MIM: 604277) account for about 40% of AD-HSP,[8] and homozygous or compound-heterozygous mutations in *SPG11* (MIM: 610844) are the most common cause of AR-HSP.[4] Both genes are thought to be involved in endosomal trafficking, and other HSP-related genes are involved in different pathways, such as mitochondrial regulation, lipid metabolism, and regulation of the endoplasmic reticulum, as was previously

[1]Montreal Neurological Institute and Hospital, McGill University, Montréal, QC H3A 2B4, Canada; [2]Department of Human Genetics, McGill University, Montréal, QC H3A 0G4, Canada; [3]Department of Neurology and Neurosurgery, McGill University, Montréal, QC H3A 0G4, Canada; [4]Equipe de Recherche sur les Maladies Neurodégénératives, Medical School and Pharmacy, Mohammed V University, Rabat, BP 6527, Morocco; [5]Service de Neurophysiologie Clinique, Hôpital des Spécialités, Centre Hospitalier Ibn Sina, Université Mohammed V Souissi, Rabat, BP 6527, Morocco; [6]Centre de Recherche, Centre Hospitalier de l'Université de Montréal, Montréal, QC H2X 0A9, Canada; [7]Département de Pathologie et Biologie Cellulaire, Université de Montréal, Montréal, QC H3C 3J7, Canada; [8]Department of Pediatrics, Neuroscience and Mental Health Institute, University of Alberta, Edmonton, AB T6G 2R3, Canada; [9]Département de Neurosciences, Université de Montréal, Montréal, QC H3C 3J7, Canada; [10]Schulich School of Medicine and Dentistry, Western University, London, ON N6A 5C1, Canada; [11]Division of Neurology, Department of Pediatrics, University of Toronto, The Hospital for Sick Children, Toronto, ON M5G 1X8, Canada; [12]Division of Clinical and Metabolic Genetics, Department of Pediatrics, University of Toronto, The Hospital for Sick Children, Toronto, ON M5G 1X8, Canada; [13]Division of Neurology, Centre Hospitalier Universitaire de Québec, and Faculty of Medicine, Laval University, Quebec City, QC G1V 0A6, Canada; [14]Division of Neurology, University of Alberta, Edmonton, AB T6G 2R3, Canada
[15]These authors contributed equally to the work
*Correspondence: guy.rouleau@mcgill.ca
http://dx.doi.org/10.1016/j.ajhg.2016.04.002.

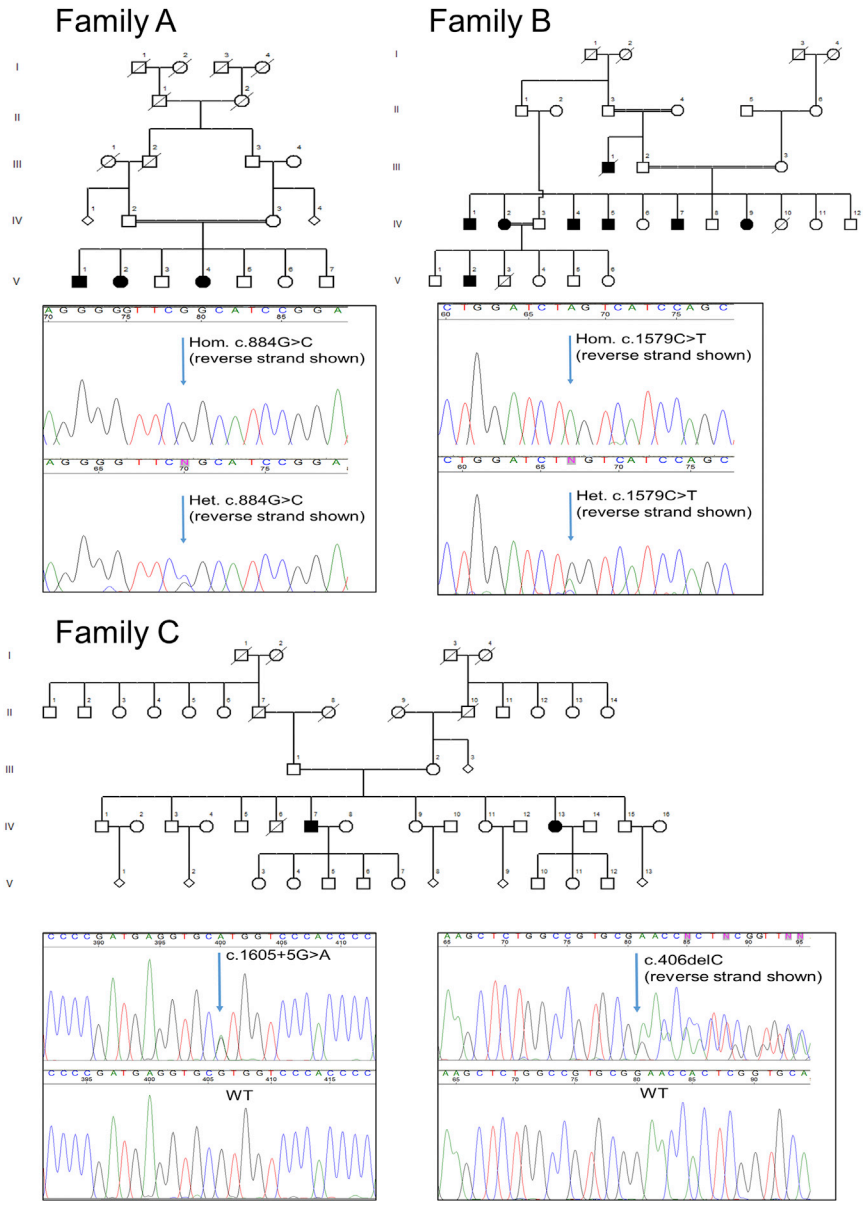

Figure 1. Pedigrees and Mutations Detected in Three Families Affected by *CAPN1*-Associated HSP

The three affected individuals from family A were homozygous for the c.884G>C (p.Arg295Pro) mutation, and all unaffected individuals with available DNA (IV-2, IV-3, V3, and V6) were heterozygous carriers of the mutation. In family B, all four affected individuals with available DNA (IV-1, IV-2, IV-5, and IV-9) were homozygous for the c.1579C>T stop variant (p.Gln527*), and all unaffected individuals with available DNA (III-2, III-3, and IV-11) were heterozygous carriers of the mutation. In family C, the two affected individuals were compound heterozygous for the frameshift c.406delC (p.Pro136Argfs*40) mutation and the splicing c.1605+5G>A mutation. Four more unaffected individuals were sequenced: III-1 (father of the affected individuals), III-2 (mother), IV-9 (sister), and IV-15 (brother). III-1 was heterozygous for the c.1605+5G>A mutation and a non-carrier of the frameshift mutation, and III-2 was heterozygous for the c.406delC mutation and a non-carrier of the splicing mutation. IV-9 was a non-carrier of both mutations, and IV-15 was a carrier of the c.1605+5G>A mutation and a non-carrier of the frameshift mutation.

reviewed.[3,6] In the current study, we used whole-exome sequencing (WES) to analyze three families affected by AR-HSP and identified homozygous or compound-heterozygous mutations in *CAPN1* (MIM: 114220) as the cause of HSP in these families. We further studied the effects of loss of function of *CAPN1* orthologs in *Caenorhabditis elegans*, *Drosophila melanogaster*, and *Danio rerio* models.

The three families (Figure 1) included two consanguineous Moroccan families (families A and B) and one family from Idaho and Utah (family C). Of note, the pedigree of family B is pseudo-dominant as a result of multiple intra-familial marriages. They live in a small village in northwestern Morocco, where many of the residents are related because of common ancestors. The clinical data on the affected individuals from these three families are detailed in Table 1. Families A and B were diagnosed and followed up by a neurologist in the Department of Clinical Neurophysiology at Centre Hospitalier Ibn Sina (Morocco), and members from family C were diagnosed and followed up by neurologists from Idaho and Utah. All individuals signed an informed-consent form before entering the study, and the study design and protocols were approved by the institutional review boards. Table 1 details the clinical characteristics of eight individuals with available clinical data, and detailed case reports are provided in the Supplemental Note. The average age at onset was 28.5 years (±8.05, range = 19–39), and the affected individuals presented with symptoms of complicated HSP. In addition to showing lower-extremity spasticity and hyperreflexia, seven of the eight individuals had upper-extremity hyperreflexia, six had dysarthria, and three had ataxia. Six individuals had foot deformities—five with the typical pes cavus and one with pes valgus. Abnormal bladder function was reported in two individuals. No seizures were reported. Overall, the motor impairment was mild to moderate, and two of the individuals (IV-2 in family B and IV-13 in family C) had started using a cane to aid walking. No vision abnormalities were reported or identified in the neurological examinations. Blood samples for DNA analysis were available from nine affected individuals (V-1, V-2, and V-4 in family A, IV-1, IV-2, IV-5, and IV-9 in family B, and IV-7 and IV-13 in family C; Figure 1), and all nine samples went through

Table 1. Clinical Features of the Affected Individuals with Autosomal-Recessive HSP and Available Clinical Data

	Family A	Family B					Family C	
	V-2	IV-1	IV-2	IV-4	IV-5	IV-9	IV-7	IV-13
Age at onset (years)	20	35	36	22	39	24	33	19
Age at examination (years)	31	47	44	42	40	30	35	22
Lower-extremity spasticity	+	+	+	+	+	+	+	+
Lower-extremity weakness	+	+	+	+	−	−	?	+
Lower-extremity hyperreflexia	+	+	+	+	+	+	?	+
Extensor plantar response	+	+	+	+	−	+	−	+
Abnormal bladder function	+	−	−	−	−	−	−	+
Foot deformity	+[a]	−	+[b]	+[b]	−	+[b]	+[b]	+[b]
Ataxia	−	−	+	−	+	−	−	+
Other symptoms and signs	dysarthria, upper-extremity hyperreflexia	dysarthria, upper-extremity hyperreflexia, sensory abnormalities, peripheral neuropathy	dysarthria, upper-extremity hyperreflexia, peripheral neuropathy, gait ataxia, upper-extremity ataxia, scoliosis	dysarthria, upper-extremity hyperreflexia, amyotrophy	ocular movement abnormalities, dysarthria, upper-extremity hyperreflexia and gait ataxia, amyotrophy	dysarthria, upper-extremity hyperreflexia	ankle clonus	mild gait ataxia, upper-extremity hyperreflexia, bilateral ankle clonus

[a]Pes valgus.
[b]Pes cavus.

WES. Additional samples from unaffected individuals were available from four individuals in family A (IV-2, IV-3, V-3, and V-6), three individuals in family B (III-2, III-3, and IV-11), and four individuals in family C (III-1, III-2, IV-9, and IV-15). These additional samples were used for validation and segregation analysis of the mutations. DNA was extracted according to a standard salting-out protocol and was captured for WES with the Agilent SureSelect Human All Exon V4 Kit according to the manufacturer's (Agilent Technologies) instructions. The captured DNA was sequenced with an Illumina HiSeq 2000 (2 × 100 bp, three samples per lane) at the Innovation Genome Center of McGill University and Genome Québec. Sequence processing, alignment, and variant calling were performed with the Burrows-Wheeler Aligner,[9] the Genome Analysis Toolkit (v.4),[10] and ANNOVAR.[11] After annotation, data on the detected variants were extracted from publicly available databases: the 1000 Genomes Project,[12] the National Heart, Lung, and Blood Institute Exome Sequencing Project (ESP) Exome Variant Server (EVS), the Exome Aggregation Consortium (ExAC) Browser, and dbSNP132. In addition, the frequencies of these variants were calculated in our in-house dataset of over 1,600 samples that had undergone WES. To estimate the potential effects of the mutation, we used the online prediction and conservation tools SIFT,[13] PolyPhen-2,[14] MutationTaster,[15] PhyloP,[16] and GERP++.[17] Details on the filtering process can be found in the Table S2. In order to validate and examine segregation of the candidate mutations with the disease, we used specific primers to amplify DNA from all affected and unaffected family members with available samples and sequenced them by Sanger sequencing (Applied Biosystem's 3730xl DNA Analyzer technology; primers are detailed in Table S1).

The average coverage of the nine samples that were sequenced by WES was 129×, 99% of the bases had a coverage > 10×, and 97% had a coverage > 20×. In order to identify potential causative mutations, we excluded all variants with an allele frequency > 0.005 in the 1000 Genomes Project, EVS, or dbSNP132 and variants that were already found in our in-house dataset. In an effort to include only nonsynonymous, frameshift, stop, and splice-site mutations, we subsequently removed synonymous, 5′ UTR, 3′ UTR, and intronic variants that were not within the six nucleotides at splice sites. Further filtering was done on the basis of predicted deleterious effects and conservation. In families A and B, homozygous mutations were considered, and in family C, both homozygous and compound-heterozygous variants were considered (Table S2). No mutations in exons covered by the exome sequencing in known or suspected HSP-associated genes segregated with the disease in any of the families. In the three families, mutations in only one gene, *CAPN1*,

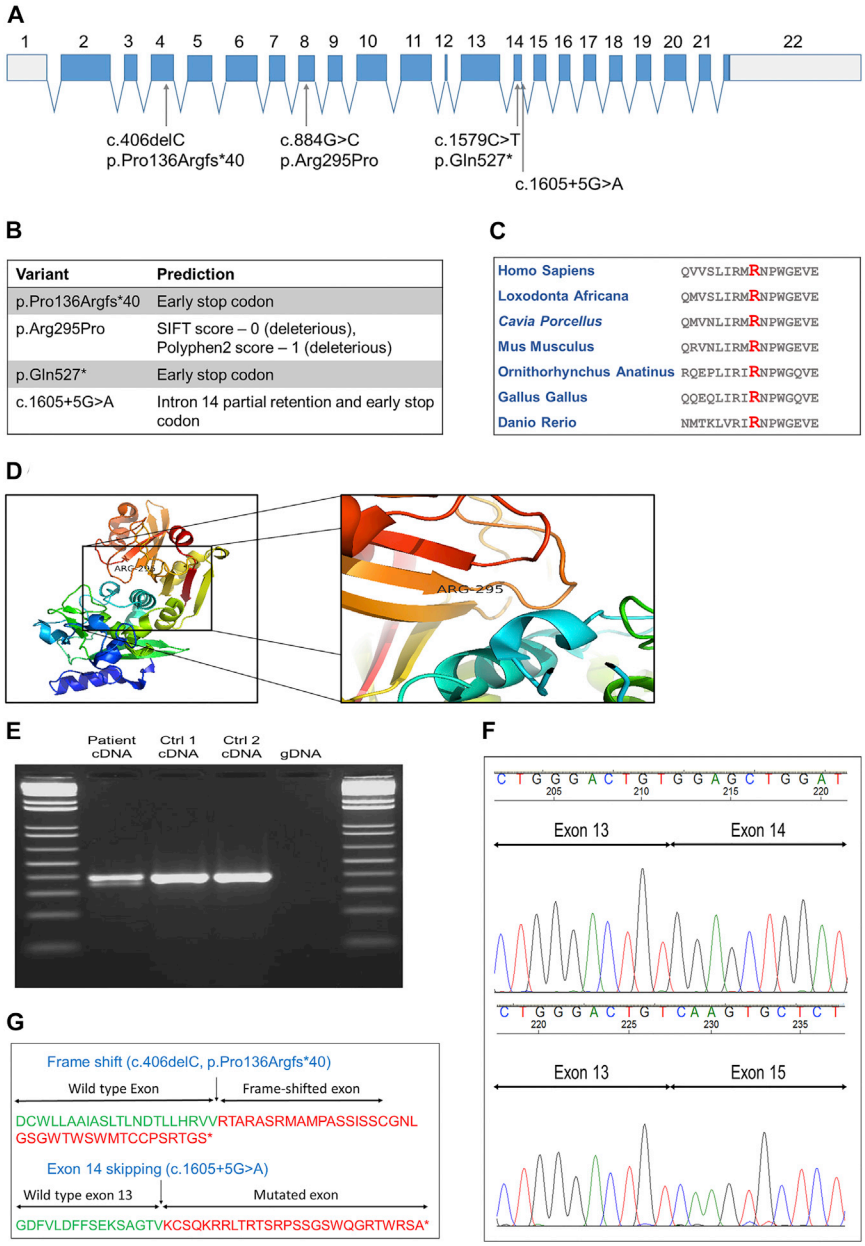

Figure 2. Characteristics and Predictions of the *CAPN1* Mutations

(A) Structure of *CAPN1* and the locations of the four mutations identified in the current study.

(B) Functional predictions of all four mutations.

(C) Conservation of Arg295 in different species. With a GERP++ score > 2, this amino acid is highly conserved.

(D) Three-dimensional model of calpain 1 and the location of the p.Arg295Pro substitution at the end of a β strand and just before the active site at p.Asn296 (PDB: 1ZCM).

(E) cDNA produced from lymphoblasts of an affected individual and two control individuals, around exon 14. In the left lane, two cDNA products were observed, suggesting that the c.1605+5G>A mutation affected splicing.

(F) Sequencing of cDNA from RT-PCR of the RNA around splicing mutation c.1605+5G>A demonstrated that this mutation caused the skipping of exon 14.

(G) Effects of the frameshift mutation c.406delC (p.Pro136Argfs*40) (top) and the splicing mutation c.1605+5G>A (bottom) on calpain 1.

segregated with the disease (spastic paraplegia 76 [SPG76 (MIM: 616907)]) after filtering (Figure 1). In family A, the three affected individuals were homozygous for a missense mutation in exon 8 of *CAPN1*: c.884G>C (GenBank: NM_005186), leading to a p.Arg295Pro substitution, which is predicted to be deleterious (SIFT score 0, PolyPhen-2 score 1) and highly conserved (GERP++ score > 2; Figure 2C). This substitution is located next to an active site in position 296, the amino acid asparagine, which is a critical Ca^{2+} binding site[18,19] at the end of a β strand (Figure 2D). In family B, the four affected individuals were homozygous for a nonsense mutation in exon 14: c.1579C>T (GenBank: NM_005186), resulting in a p.Gln527* early termination of the protein. Homozygosity mapping of the seven individuals from these two families confirmed that a region on chromosome 11, spanning 3.5 Mb and containing *CAPN1*, is the only shared homozygous region. In family C, the two affected individuals were compound heterozygous for a frameshift mutation on exon 4 (c.406delC [p.Pro136Argfs*40]; Figure 2G) and a splicing mutation (c.1605+5G>A; Figures 2E–2G). None of these variants from the three families were identified in the 1000 Genome Project, ESP, or our in-house dataset of >1,600 exome-sequencing samples. The coding variants were also not detected in the ExAC Browser, and the c.1605+5G>A splice-site mutation had a frequency of 0.0001. All mutations were validated via Sanger sequencing, and all the available DNA samples from family members were also sequenced. In family A, the two parents (IV-2 and IV-3; Figure 1) and two siblings (V-3 and V-6) of the affected individuals were all heterozygous for the *CAPN1* c.884G>C (p.Arg295Pro) mutation. In family B, the two parents (III-2 and III-3) and one sibling (IV-11) of the four individuals sequenced by WES were all heterozygous carriers of the *CAPN1* c.1579C>T (p.Gln527*) mutation. In family C, both parents (III-1 and III-2) and two siblings (IV-9 and IV-15) were sequenced. The father, III-1, was a heterozygous carrier of the c.1605+5G>A mutation, and the mother, III-2, was a heterozygous carrier of the c.406delC mutation, confirming phasing. Sibling IV-9 was a non-carrier of both variants, and IV-15 was a heterozygous carrier of the c.1605+5G>A

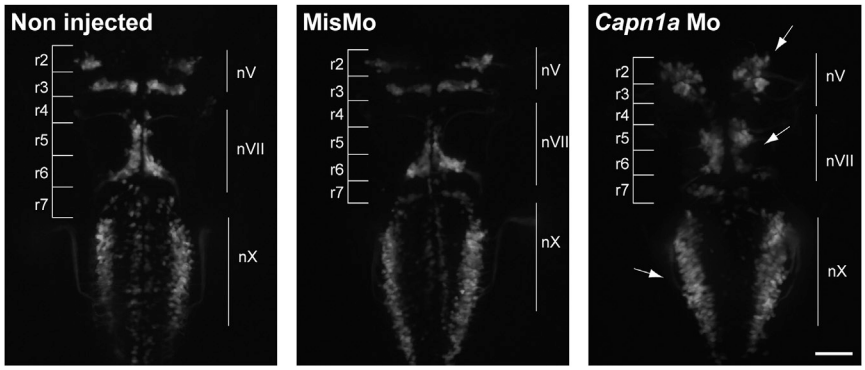

Figure 3. Branchiomotor Neurons of *capn1a*-Mo-Injected Embryos Display Abnormal Migration
Abnormal development and migration of both nV (trigeminal) and nVII (facial) branchiomotor neurons in 2 dpf Islet1:GFP embryos either not injected or injected with the mismatch Mo (MisMo) or *capn1a* Mo. Arrows indicate abnormally located cell bodies. R stands for "rhombomere." The scale bar represents 50 μm.

mutation. To examine the predicted effect of the splice-site c.1605+5G>A mutation, we produced RNA from immortalized lymphoblasts from individual IV-7 (family C) and from healthy family members, and we produced cDNA with the Invitrogen SuperScript III Reverse Transcriptase Kit (Invitrogen). Specific primers (forward 5′-ACTATTGG CTTCGCGGTCTA-3′ and reverse 5′-ATTGTCCGCAACTCC TTCAC-3′) were designed to amplify the cDNA around the c.1605+5G>A mutation with a cDNA amplicon length of 389 bp (DNA amplicon length = 3,405 bp). Individual IV-7 had two copies of cDNA with different lengths around the c.1605+5G>A splice-site mutation (Figure 2E). Sequencing of the cDNA after separation on gel demonstrated that this splice variant results in exon 14 skipping and an early stop codon (Figures 2E–2G).

RNAi knockdown of *clp-1*, the *C. elegans* ortholog of *CAPN1*, led to neurodegeneration of GABAergic motor neurons and an age-dependent paralysis phenotype (see Figure S1 for details on the experiments and results). Similarly, loss of function of the *CAPN1* ortholog in *D. melanogaster* led to locomotor defects and axonal abnormalities (see Figures S2 and S3 for details on the experiments and results). RNAi against the *D. melanogaster* ortholog, *calpain B*, led to age-dependent negative geotaxis (Figure S2). Defects in axons were observed in transgenic flies expressing *calpain B* with the pan-neuronal driver Elav. Axons appeared to have larger diameters and increased levels of acetylated tubulin (Figure S3).

Zebrafish (*D. rerio*) embryos were collected and staged according to standard methods.[20] The local animal care committee at the Centre de Recherche du Centre Hospitalier de l'Université de Montréal, having received the protocol relevant to this project and relating to animal care and treatment, certified that the care and treatment of animals was in accordance with the guidelines and principles of the Canadian Council on Animal Care. Zebrafish embryos (no adults were used) are insentient to pain. Similarly to the findings in *D. melanogaster*, Figure S4 demonstrates clusters of acetylated tubulin in zebrafish with mutant *calpain 1a* (*capn1a*). Increased acetylated tubulin is associated with hyperstabilization of microtubules and has previously been associated with *SPAST* mutations. Zebrafish *capn1a* and *calpain 1b* (*capn1b*) both encode proteins that are orthologs of the human CAPN1.[21] We used a morpholino oligonucleotide (Mo) against each gene to model the loss of function of *CAPN1*. The *capn1a* Mo, but not the *capn1b* Mo, led to a phenotype (data not shown). Details on the knockdown of the zebrafish calpains, morphology measurements, and imaging are in Figure S5 legend. The *capn1a* Mo resulted in several developmental defects visible at 2 days postfertilization (dpf), and a moderate to severe phenotype was exhibited by 78% of injected embryos at 5 dpf, indicating that these defects are long lasting (Figure S5). Knockdown with the *capn1a* Mo was confirmed in western blots at 48 hr postfertilization (hpf) (Figure S6). However, co-injecting the human wild-type *CAPN1* mRNA (up to 500 pg of RNA) in wild-type and Mo-injected eggs failed to show a toxic effect of the RNA on its own or a rescue of the Mo-induced phenotype. By western blotting (Figure S6), the zebrafish and human calpain 1 proteins showed exclusive patterns that explain the failed rescue. Specifically, the human protein was detected at 24 hpf, but not at 48 hpf, whereas the zebrafish protein was detected only later at 48 hpf. Thus, the early expression of human mRNA could very well have failed to rescue the later knockdown phenotype. Because of the lack of rescue, the role of the CAPN1 p.Arg295Pro substitution could not be established in this model, and other models will be necessary for examining the effect of this substitution. Because *capn1a* is mainly expressed in the brain starting at 24 hpf,[21] we injected *capn1a* Mo in the Islet1::GFP transgenic fish expressing GFP in the motor neurons, including the branchiomotor neurons. We observed a disorganization of these motor neurons in comparison to those of the control, as well as migration defects of the nV trigeminal nuclei in rhombomeres 2 and 3 (r2 and r3, respectively) and of the VII facial branchiomotor neuronal cell bodies, which had not fully migrated from r4 to r6. Furthermore, the vagal motor neurons had an aberrant positioning and spacing, probably because of a defect in cell motility (Figure 3).

Growing axons in the brain and spinal cord were then observed with an antibody against acetylated tubulin. The microtubule network in the brain of *capn1a*-Mo-injected embryos (Figures 4B and 4D) appeared to be following a different pattern than in the morphants injected with

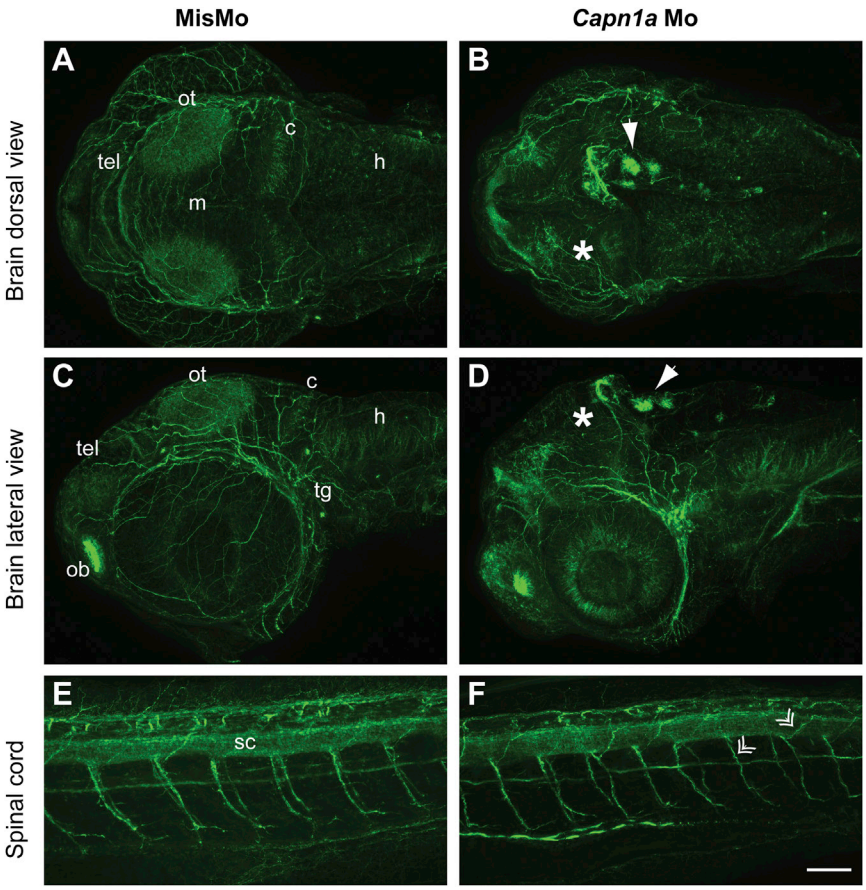

Figure 4. Disorganization of the Microtubule Network in the Brain of *capn1a* Morphants

(A and B) Dorsal view of Z-projections of acetylated-tubulin staining in the brain of embryos injected with MisMo (A) and *capn1a* Mo (B).

(C and D) Lateral view of Z-projections of acetylated-tubulin staining in the brain of embryos injected with MisMo (C) and *capn1a* Mo (D). The dorsal side is toward the top of the image.

(E and F) Spinal cord, along the six to eight somites spanning the anus of the embryos, of embryos injected with MisMo (E) and *capn1a* Mo (F). The dorsal side is toward the top of the image. Double arrows point toward thinner and disorganized motor neuron axons of the *capn1a* morphants. Solid white arrows show the clusters of tubulin. Asterisks show the fainter staining of the optic tectum of *capn1a* morphants. In all images, caudal is to the left. The scale bar represents 60 μm. Abbreviations are as follows: ot, optic tectum; tg, trigeminal ganglion; h, hindbrain; c, cerebellum; m, midbrain; tel, telencephalon; ob, olfactory bulb; and sc, spinal cord.

mismatch Mo (MisMo) (Figures 4A and 4C). Reduced acetylated-tubulin staining could be observed at the level of the optic tectum and cerebellum, whereas a stronger staining was found in the telencephalon. Strikingly, clusters of acetylated tubulin could be observed in some cells in the dorsalmost part of the brain (Figures 4B and 4D). Furthermore, acetylated-tubulin staining in the spinal cord demonstrated that microtubules in the motor neuron axons were thinner and more disorganized, although this effect was not as strong as in the brain (Figures 4E and 4F). Although the exact pattern varied from embryo to embryo, the vast majority of embryos injected with the *capn1a* Mo (29/30) exhibited similar staining, whereas the controls did not (both non-injected embryos [0/30, data not shown] and MisMo-injected embryos [0/30]).

The current study demonstrates that rare homozygous or compound-heterozygous mutations in *CAPN1* cause a complicated form of HSP. Most of the affected individuals from the three families suffer from additional neurological symptoms in addition to the typical spasticity of the lower limbs, such as upper-extremity hyperreflexia, dysarthria, and gait ataxia (Table 1). These features are also seen in other autosomal-recessive forms of HSP. For example, individuals with AR-HSP caused by mutations in *SPG7* (MIM: 607259) often present with phenotypes very similar to those described in the current study, including symptoms such as dysarthria, ataxia, upper-extremity hyperreflexia, amyotrophy, pes cavus, and sensory neuropathy.[22–24] Similar phenotypes have also been observed in individuals with mutations in *KIF1A* (MIM: 610357)[25,26] and other forms of AR-HSP.[27] In our dataset that includes 405 HSP-affected individuals from 252 families, *CAPN1* mutations account for 2.2% of the affected individuals and 1.2% of the families. However, this is an overestimation, given that our dataset does not include families in whom the genetic cause was established prior to our study. Therefore, these values should be considered as maximal. *CAPN1*, located in chromosomal region 11q13, encodes calpain 1, also known as the large subunit of μ-calpain, a calcium-activated cysteine protease that is widely present in the CNS.[28] Calpain 1 is probably important for several functions in the CNS, but its exact role in humans is still not clear. Calpain 1 is involved in synaptic plasticity,[29–32] and several mechanisms for its function have been suggested in animal models. For example, it was shown that calpain interacts with CDK5 and NR2B to control NMDA-receptor degradation and synaptic plasticity.[33] Another study suggested that calpain 1 can affect synaptic plasticity through degradation of its substrate, glutamate receptor-interacting protein, thus affecting AMPA receptors.[34] However, there are contradicting results regarding the roles of calpains in neuroprotection and neurodegeneration, given that several studies suggest that calpain inhibition might be neuroprotective.[35,36] A recent study might offer a solution for this contradiction by demonstrating that selective knockout of *Capn1* (encoding μ-calpain) leads to increased neurotoxicity and that its activity is in fact neuroprotective, whereas

knockout of *Capn2* (encoding m-calpain) is neuroprotective.[37] Our animal models support the neuroprotective role of *calpain 1*, given that its knockdown led to neurodegeneration or disorganization of neurons. Therefore, it is likely that different forms of calpain have different or even opposing effects on neurodegeneration and that calpains might have different effects in different disorders and different species.

This can be further exemplified by calpain-1-deficient mice, which have normal gross brain development and architecture yet have reduced spine density and ramifications of basal and apical dendrites in hippocampal CA1 pyramidal neurons, emphasizing the importance of calpain 1 in regulation and organization of dendritic trees in hippocampal CA1 neurons.[38] Moreover, a knockout mouse model of another HSP-related gene, *CYP7B1* (MIM: 270800), also resulted in the lack of an obvious CNS phenotype.[39] These observations are comparable to human HSP, because in humans too, brain imaging and development often seem to be normal, whereas affected individuals in fact suffer from axonal degeneration of the descending corticospinal tract and ascending sensory fibers.[5] Interestingly, loss-of-function mutations in *CAPN1* have been suggested to cause spinocerebellar ataxia in dogs,[40] a neurological disorder that shares features with HSP. Of note, all but one of the individuals in our studies have cerebellar signs such as dysarthria and ataxia.

In zebrafish embryos, knockdown of *calpain 1a* resulted in disruption of brain development, particularly of branchiomotor neuron migration and positioning. The microtubule network in the brain was disorganized, such that some regions showed an abnormal accumulation of axonal acetylated tubulin, whereas others were depleted. This disruption of the microtubule network was more prominent in the brain, but motor neuron axons in the spinal cord were also moderately affected. The presence of large clusters of acetylated tubulin in some cells of the brain is specific to the knockdown of *calpain 1a*, given that it was not observed in other embryos exhibiting hydrocephalus and migration defects in branchiomotor neurons.[41,42] Similarly, the neuromuscular junction of *D. melanogaster* with *calpain B* knockdown showed abnormal levels of acetylated tubulin. Interestingly, similar observations were reported for spastin, encoded by *SPAST*, in which mutations are the most common genetic cause of HSP.[43,44] This suggests that the two genes might be involved in a similar mechanism; however, whether *CAPN1*- and *SPG4*-associated HSP share the same mechanisms is still to be determined.

Fully understanding the roles of the different calpains in general, and calpain 1 specifically, will require more studies, especially in human tissues. Such studies should focus on isolating the effects of specific calpains on neurodegeneration and neuroprotection. In addition, efforts should be made to identify more individuals with *CAPN1*-associated HSP to expand our knowledge of its phenotype.

Supplemental Data

Supplemental Data include a Supplemental Note, six figures, and three tables and can be found with this article online at http://dx.doi.org/10.1016/j.ajhg.2016.04.002.

Acknowledgments

We thank the families for their participation. This study was funded by an Emerging Team Grant (RN127580-260005) from the Canadian Institutes for Health Research (CIHR) in collaboration with the Canadian Organization for Rare Disorders. This work was done as a part of a Canadian collaboration to study hereditary spastic paraplegia (CanHSP). Z.G.-O. is supported by a postdoctoral fellowship from the CIHR. P.D. holds a Canada Research Chair in Neuroscience, and A.L. is the recipient of a CIHR ALS Canada Doctoral Research Award. G.A.R. holds a Canada Research Chair in Genetics of the Nervous System and the Wilder Penfield Chair in Neurosciences. We thank Dr. Hitoshi Okamoto for the zebrafish Islet-1 transgenic line. We thank Helene Catoire, Pascale Hince, Cynthia Bourassa, Amirthagowri Ambalavanan, and Cathy Mirarchi for their assistance.

Received: October 18, 2015
Accepted: April 5, 2016
Published: May 5, 2016

Web Resources

dbSNP132, http://www.ncbi.nlm.nih.gov/projects/SNP/snp_summary.cgi?build_id=132
ExAC Browser, http://exac.broadinstitute.org/
GERP++, http://mendel.stanford.edu/SidowLab/downloads/gerp/
MutationTaster, http://www.mutationtaster.org/
NHLBI Exome Sequencing Project (ESP) Exome Variant Server, http://evs.gs.washington.edu/EVS/
OMIM, http://www.omim.org/
PhyloP, http://compgen.cshl.edu/phast/
PolyPhen-2, http://genetics.bwh.harvard.edu/pph2/
RefSeq, http://www.ncbi.nlm.nih.gov/refseq/
SIFT, http://sift.jcvi.org/

References

1. McDermott, C., White, K., Bushby, K., and Shaw, P. (2000). Hereditary spastic paraparesis: a review of new developments. J. Neurol. Neurosurg. Psychiatry *69*, 150–160.
2. Salinas, S., Proukakis, C., Crosby, A., and Warner, T.T. (2008). Hereditary spastic paraplegia: clinical features and pathogenetic mechanisms. Lancet Neurol. *7*, 1127–1138.
3. Blackstone, C. (2012). Cellular pathways of hereditary spastic paraplegia. Annu. Rev. Neurosci. *35*, 25–47.
4. Lo Giudice, T., Lombardi, F., Santorelli, F.M., Kawarai, T., and Orlacchio, A. (2014). Hereditary spastic paraplegia: clinical-genetic characteristics and evolving molecular mechanisms. Exp. Neurol. *261*, 518–539.
5. Deluca, G.C., Ebers, G.C., and Esiri, M.M. (2004). The extent of axonal loss in the long tracts in hereditary spastic paraplegia. Neuropathol. Appl. Neurobiol. *30*, 576–584.
6. Noreau, A., Dion, P.A., and Rouleau, G.A. (2014). Molecular aspects of hereditary spastic paraplegia. Exp. Cell Res. *325*, 18–26.

7. Novarino, G., Fenstermaker, A.G., Zaki, M.S., Hofree, M., Silhavy, J.L., Heiberg, A.D., Abdellateef, M., Rosti, B., Scott, E., Mansour, L., et al. (2014). Exome sequencing links corticospinal motor neuron disease to common neurodegenerative disorders. Science *343*, 506–511.
8. Hazan, J., Fonknechten, N., Mavel, D., Paternotte, C., Samson, D., Artiguenave, F., Davoine, C.S., Cruaud, C., Dürr, A., Wincker, P., et al. (1999). Spastin, a new AAA protein, is altered in the most frequent form of autosomal dominant spastic paraplegia. Nat. Genet. *23*, 296–303.
9. Li, H., and Durbin, R. (2009). Fast and accurate short read alignment with Burrows-Wheeler transform. Bioinformatics *25*, 1754–1760.
10. McKenna, A., Hanna, M., Banks, E., Sivachenko, A., Cibulskis, K., Kernytsky, A., Garimella, K., Altshuler, D., Gabriel, S., Daly, M., and DePristo, M.A. (2010). The Genome Analysis Toolkit: a MapReduce framework for analyzing next-generation DNA sequencing data. Genome Res. *20*, 1297–1303.
11. Wang, K., Li, M., and Hakonarson, H. (2010). ANNOVAR: functional annotation of genetic variants from high-throughput sequencing data. Nucleic Acids Res. *38*, e164.
12. Abecasis, G.R., Auton, A., Brooks, L.D., DePristo, M.A., Durbin, R.M., Handsaker, R.E., Kang, H.M., Marth, G.T., and McVean, G.A.; 1000 Genomes Project Consortium (2012). An integrated map of genetic variation from 1,092 human genomes. Nature *491*, 56–65.
13. Kumar, P., Henikoff, S., and Ng, P.C. (2009). Predicting the effects of coding non-synonymous variants on protein function using the SIFT algorithm. Nat. Protoc. *4*, 1073–1081.
14. Adzhubei, I.A., Schmidt, S., Peshkin, L., Ramensky, V.E., Gerasimova, A., Bork, P., Kondrashov, A.S., and Sunyaev, S.R. (2010). A method and server for predicting damaging missense mutations. Nat. Methods *7*, 248–249.
15. Schwarz, J.M., Cooper, D.N., Schuelke, M., and Seelow, D. (2014). MutationTaster2: mutation prediction for the deep-sequencing age. Nat. Methods *11*, 361–362.
16. Pollard, K.S., Hubisz, M.J., Rosenbloom, K.R., and Siepel, A. (2010). Detection of nonneutral substitution rates on mammalian phylogenies. Genome Res. *20*, 110–121.
17. Davydov, E.V., Goode, D.L., Sirota, M., Cooper, G.M., Sidow, A., and Batzoglou, S. (2010). Identifying a high fraction of the human genome to be under selective constraint using GERP++. PLoS Comput. Biol. *6*, e1001025.
18. Khorchid, A., and Ikura, M. (2002). How calpain is activated by calcium. Nat. Struct. Biol. *9*, 239–241.
19. Moldoveanu, T., Hosfield, C.M., Lim, D., Elce, J.S., Jia, Z., and Davies, P.L. (2002). A Ca(2+) switch aligns the active site of calpain. Cell *108*, 649–660.
20. Kimmel, C.B., Ballard, W.W., Kimmel, S.R., Ullmann, B., and Schilling, T.F. (1995). Stages of embryonic development of the zebrafish. Dev. Dyn. *203*, 253–310.
21. Lepage, S.E., and Bruce, A.E. (2008). Characterization and comparative expression of zebrafish calpain system genes during early development. Dev. Dyn. *237*, 819–829.
22. Casari, G., and Marconi, R. (1993). Spastic Paraplegia 7. In GeneReviews, R.A. Pagon, M.P. Adam, H.H. Ardinger, S.E. Wallace, A. Amemiya, L.J.H. Bean, T.D. Bird, C.R. Dolan, C.T. Fong, R.J.H. Smith, et al., eds.
23. Wilkinson, P.A., Crosby, A.H., Turner, C., Bradley, L.J., Ginsberg, L., Wood, N.W., Schapira, A.H., and Warner, T.T. (2004). A clinical, genetic and biochemical study of SPG7 mutations in hereditary spastic paraplegia. Brain *127*, 973–980.
24. Brugman, F., Scheffer, H., Wokke, J.H., Nillesen, W.M., de Visser, M., Aronica, E., Veldink, J.H., and van den Berg, L.H. (2008). Paraplegin mutations in sporadic adult-onset upper motor neuron syndromes. Neurology *71*, 1500–1505.
25. Klebe, S., Azzedine, H., Durr, A., Bastien, P., Bouslam, N., Elleuch, N., Forlani, S., Charon, C., Koenig, M., Melki, J., et al. (2006). Autosomal recessive spastic paraplegia (SPG30) with mild ataxia and sensory neuropathy maps to chromosome 2q37.3. Brain *129*, 1456–1462.
26. Klebe, S., Lossos, A., Azzedine, H., Mundwiller, E., Sheffer, R., Gaussen, M., Marelli, C., Nawara, M., Carpentier, W., Meyer, V., et al. (2012). KIF1A missense mutations in SPG30, an autosomal recessive spastic paraplegia: distinct phenotypes according to the nature of the mutations. Eur. J. Hum. Genet. *20*, 645–649.
27. Coutinho, P., Barros, J., Zemmouri, R., Guimarães, J., Alves, C., Chorão, R., Lourenço, E., Ribeiro, P., Loureiro, J.L., Santos, J.V., et al. (1999). Clinical heterogeneity of autosomal recessive spastic paraplegias: analysis of 106 patients in 46 families. Arch. Neurol. *56*, 943–949.
28. Goll, D.E., Thompson, V.F., Li, H., Wei, W., and Cong, J. (2003). The calpain system. Physiol. Rev. *83*, 731–801.
29. Lynch, G., and Baudry, M. (1984). The biochemistry of memory: a new and specific hypothesis. Science *224*, 1057–1063.
30. Denny, J.B., Polan-Curtain, J., Ghuman, A., Wayner, M.J., and Armstrong, D.L. (1990). Calpain inhibitors block long-term potentiation. Brain Res. *534*, 317–320.
31. Vanderklish, P., Bednarski, E., and Lynch, G. (1996). Translational suppression of calpain blocks long-term potentiation. Learn. Mem. *3*, 209–217.
32. Zadran, S., Jourdi, H., Rostamiani, K., Qin, Q., Bi, X., and Baudry, M. (2010). Brain-derived neurotrophic factor and epidermal growth factor activate neuronal m-calpain via mitogen-activated protein kinase-dependent phosphorylation. J. Neurosci. *30*, 1086–1095.
33. Hawasli, A.H., Benavides, D.R., Nguyen, C., Kansy, J.W., Hayashi, K., Chambon, P., Greengard, P., Powell, C.M., Cooper, D.C., and Bibb, J.A. (2007). Cyclin-dependent kinase 5 governs learning and synaptic plasticity via control of NMDAR degradation. Nat. Neurosci. *10*, 880–886.
34. Lu, X., Wyszynski, M., Sheng, M., and Baudry, M. (2001). Proteolysis of glutamate receptor-interacting protein by calpain in rat brain: implications for synaptic plasticity. J. Neurochem. *77*, 1553–1560.
35. O'Hanlon, G.M., Humphreys, P.D., Goldman, R.S., Halstead, S.K., Bullens, R.W., Plomp, J.J., Ushkaryov, Y., and Willison, H.J. (2003). Calpain inhibitors protect against axonal degeneration in a model of anti-ganglioside antibody-mediated motor nerve terminal injury. Brain *126*, 2497–2509.
36. Crocker, S.J., Smith, P.D., Jackson-Lewis, V., Lamba, W.R., Hayley, S.P., Grimm, E., Callaghan, S.M., Slack, R.S., Melloni, E., Przedborski, S., et al. (2003). Inhibition of calpains prevents neuronal and behavioral deficits in an MPTP mouse model of Parkinson's disease. J. Neurosci. *23*, 4081–4091.
37. Wang, Y., Briz, V., Chishti, A., Bi, X., and Baudry, M. (2013). Distinct roles for μ-calpain and m-calpain in synaptic NMDAR-mediated neuroprotection and extrasynaptic NMDAR-mediated neurodegeneration. J. Neurosci. *33*, 18880–18892.
38. Amini, M., Ma, C.L., Farazifard, R., Zhu, G., Zhang, Y., Vanderluit, J., Zoltewicz, J.S., Hage, F., Savitt, J.M., Lagace, D.C., et al. (2013). Conditional disruption of calpain in the CNS alters

dendrite morphology, impairs LTP, and promotes neuronal survival following injury. J. Neurosci. *33*, 5773–5784.
39. Li-Hawkins, J., Lund, E.G., Turley, S.D., and Russell, D.W. (2000). Disruption of the oxysterol 7alpha-hydroxylase gene in mice. J. Biol. Chem. *275*, 16536–16542.
40. Forman, O.P., De Risio, L., and Mellersh, C.S. (2013). Missense mutation in CAPN1 is associated with spinocerebellar ataxia in the Parson Russell Terrier dog breed. PLoS ONE *8*, e64627.
41. Chen, H.L., Yuh, C.H., and Wu, K.K. (2010). Nestin is essential for zebrafish brain and eye development through control of progenitor cell apoptosis. PLoS ONE *5*, e9318.
42. Hanington, P.C., Patten, S.A., Reaume, L.M., Waskiewicz, A.J., Belosevic, M., and Ali, D.W. (2008). Analysis of leukemia inhibitory factor and leukemia inhibitory factor receptor in embryonic and adult zebrafish (Danio rerio). Dev. Biol. *314*, 250–260.
43. Denton, K.R., Lei, L., Grenier, J., Rodionov, V., Blackstone, C., and Li, X.J. (2014). Loss of spastin function results in disease-specific axonal defects in human pluripotent stem cell-based models of hereditary spastic paraplegia. Stem Cells *32*, 414–423.
44. Trotta, N., Orso, G., Rossetto, M.G., Daga, A., and Broadie, K. (2004). The hereditary spastic paraplegia gene, spastin, regulates microtubule stability to modulate synaptic structure and function. Curr. Biol. *14*, 1135–1147.